Shock Waves (1993) 3: 49–53

Shock Waves

Absolute intensity measurements of impurity emissions in a shock tunnel and their consequences for laser-induced fluorescence experiments

P.C. Palma, A.F.P Houwing and R.J. Sandeman

Department of Physics and Theoretical Physics, Faculty of Science, Australian National University, GPO Box 4, Canberra, 2601, Australia

Received October 7, 1992; Accpeted November 23, 1992

Abstract. Absolute intensity measurements of impurity emissions in a shock tunnel nozzle flow are presented. The impurity emission intensities were measured with a photomultiplier and optical multichannel analyser and calibrated against an intensity standard. The various metallic contaminants were identified and their intensities measured in the spectral regions 290 to 330 nm and 375 to 385 nm. A comparison with calculated fluorescence intensities for predissociated laser-induced fluorescence signals is made. It is found that the emission background is negligible for most fluorescence experiments.

Key words: Laser-induced predissociation fluorescence, Shock tunnel impurities, Absolute intensity measurements

1. Introduction

The application of optical techniques to hypervelocity flows in shock tubes allows non-intrusive measurements in regions that are otherwise difficult to access. These techniques include interferometry, absorption and emission spectroscopy, schlieren, Laser-Induced Fluorescence (LIF) (Paul et al. 1989; Meier et al. 1991; Palmer et al. 1992) and various non-linear spectroscopic schemes. Planar LIF is particularly attractive as it offers instantaneous two dimensional imaging of flow parameters such as temperature, species concentration and velocity. The major limitation of LIF is that collisional quenching affects the accuracy of this method at high temperatures and pressures. A variation of this LIF method involves using a fast predissociating upper state to reduce the possibility of a collision occurring within the predissociation lifetime (Andresen et al. 1988). However this technique significantly reduces the LIF signal intensity. It is possible that the predissociated LIF signals may be "swamped" by the background luminosity which occurs in hypervelocity flows. The experiments described in this paper were designed to measure the absolute intensities of the shock tunnel flow emissions and compare these results with theoretical calculations of predissociated LIF signals.

A major constituent of the background emissions is produced by atomic impurities which have been eroded from the interior surfaces of the shock tunnel and heated by the flow. A comprehensive study of the impurities in a free piston shock tube facility was performed by Kilpin. Iron, chromium, nickel, molybdenum, manganese and titanium were identified as well as several other trace elements. Hornung and Sandeman (1974) found by interferometric means the concentration of chromium in the ANU T3 shock tunnel to be approximately 1 in 3000.

2. Experiment

The experiment was conducted in the Free Piston Shock Tunnel T3 at the Australian National University. The shock tunnel is shown schematically in Fig. 1. A description of the shock tunnel and its operation is given by Stalker (1970, 1972). LIF experiments are planned for this facility to investigate combustion phenomena in a Supersonic Combustion Ramjet (SCRAMJET). These LIF experiments will augment studies using Coherent Anti-Stokes Raman Scattering (CARS) currently in progress (Pulford et al. 1992). Hence, the observation volume for the following emission measurements was inside the duct of a SCRAMJET model. The SCRAMJET model is as described by Stalker et al. (1984, 1988). The adjustable floor of the duct was placed in the zero degree position producing a duct of constant width (50 mm) and height (25 mm). A fused silica window (diameter 25 mm) was mounted in the top of the duct to view the flow (25 mm downstream of the hydrogen injector).

Figure 2 illustrates the optical arrangement for the experiment. The radiation from the flow was imaged with a fused silica lens ($f/2.5$) onto the entrance slit of a 1 metre spectrometer (Spex 1704 with a 1200 mm^{-1} grating). The spectrometer was positioned above the optical table for the CARS experiment, which was in progress at the time, in order to view the emissions through the top window of the test section. The optical periscope arrangement was necessary to avoid a steel girder above the test section which is

Correspondence to: A.F.P. Houwing

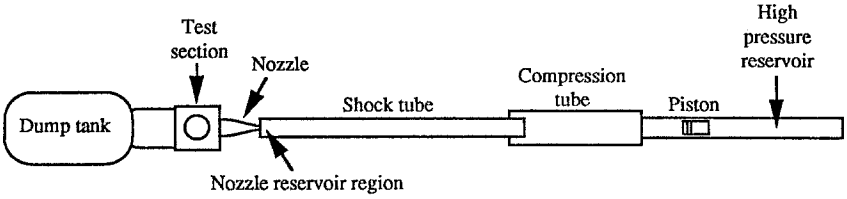

Fig. 1. The T3 free piston shock tunnel (Stalker 1970, 1972). Metallic contaminants are believed to be introduced into the flow in the high temperature nozzle reservoir region and from the surfaces exposed to the flow in the nozzle and test section regions

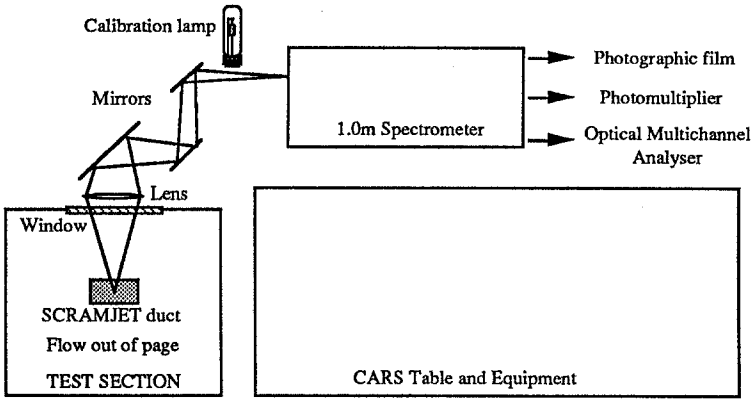

Fig. 2. Illustration of experimental arrangement. This is a view from the end of the shock tunnel with the flow coming out of the page

used to support the nozzle during set up procedures. The linear dispersion of the spectrometer was measured to be 0.83 nm mm^{-1} at 300 nm. The spectral regions of interest were from 290 to 330 nm and 375 to 385 nm which correspond to LIF emission wavelengths for molecular oxygen (Andresen et al. 1988). Pressure transducers located along the shock tube provided a method for measuring shock wave velocities and determining the triggering times for the optical experiments.

Three methods were employed to measure the spectrally dispersed impurity emissions. Photographic exposures were made with high speed infrared film (Kodak 2481) which had a maximum spectral sensitivity in the 250 nm to 400 nm spectral region. The negatives were exposed for the entire test time to ensure adequate exposure. To allow accurate calibration, a spectrum from a mercury-zinc-cadmium lamp was placed alongside the impurity spectrum by masking half the entrance slit of the spectrometer. These exposures allowed identification of the spectral lines and the various atomic species from which they originated. A photomultiplier (Thorn EMI 9783B) was used to measure the time resolved intensity of specific emission lines. The photomultiplier output signal was recorded on a digital storage oscilloscope (Tektronix 2232) and later transferred to a microcomputer. The oscilloscope was triggered at shock reflection by the nozzle reservoir pressure transducer and proceeded to collect data for approximately 2 ms. An Optical Multichannel Analyser (Princeton Applied Research OMA-2) was used to obtain spectrally dispersed intensity measurements. The OMA was gated for approximately 30 μs at different times after shock reflection. Finally, the experimental system was calibrated with an intensity standard (tungsten ribbon filament lamp from Philips).

3. Results

Table 1 shows the experimental conditions for the shock tunnel operating in shock-reflected mode with the contoured nozzle used in previous SCRAMJET studies (Stalker et al. 1984, 1988). The photographic negatives were examined with a digital readout microscope and the lines centres were measured with an accuracy of 0.01 nm. Approximately 100 lines were observed in the region from 290 to 330 nm, half were due to transitions in iron and a quarter were due to chromium transitions which are the major elements of stainless steel. Seven weaker nickel lines were also identified. Four molybdenum lines were identified including two stronger ones at 313.259 and 315.816 nm. Three lines were attributed to tin at 303.412, 317.505 and 326.234 nm and two strong aluminium lines were identified at 308.215 and 309.271 nm. Three copper lines were identified at 296.116, 324.754 and 327.396 nm. They are an order of magnitude greater than the surrounding emission lines and most likely originate from the brass hydrogen injector in the SCRAM-

Table 1. Conditions for the experiment. The compression tube was filled to 48 kPa of Helium and the reservoir was 3.7 MPa of air. The diaphragm was 1.6 mm thick (B.P. 50 MPa)

Condition	Shock tube filling pressure (kPa)	Shock speed (km/s)	Reservoir enthalpy (MJ/kg)
(a)	6.7	5.1	25
(b)	13.3	4.2	17
(c)	26.7	3.6	12
(d)	53.3	3.0	8.3
(e)	150	2.1	4.4

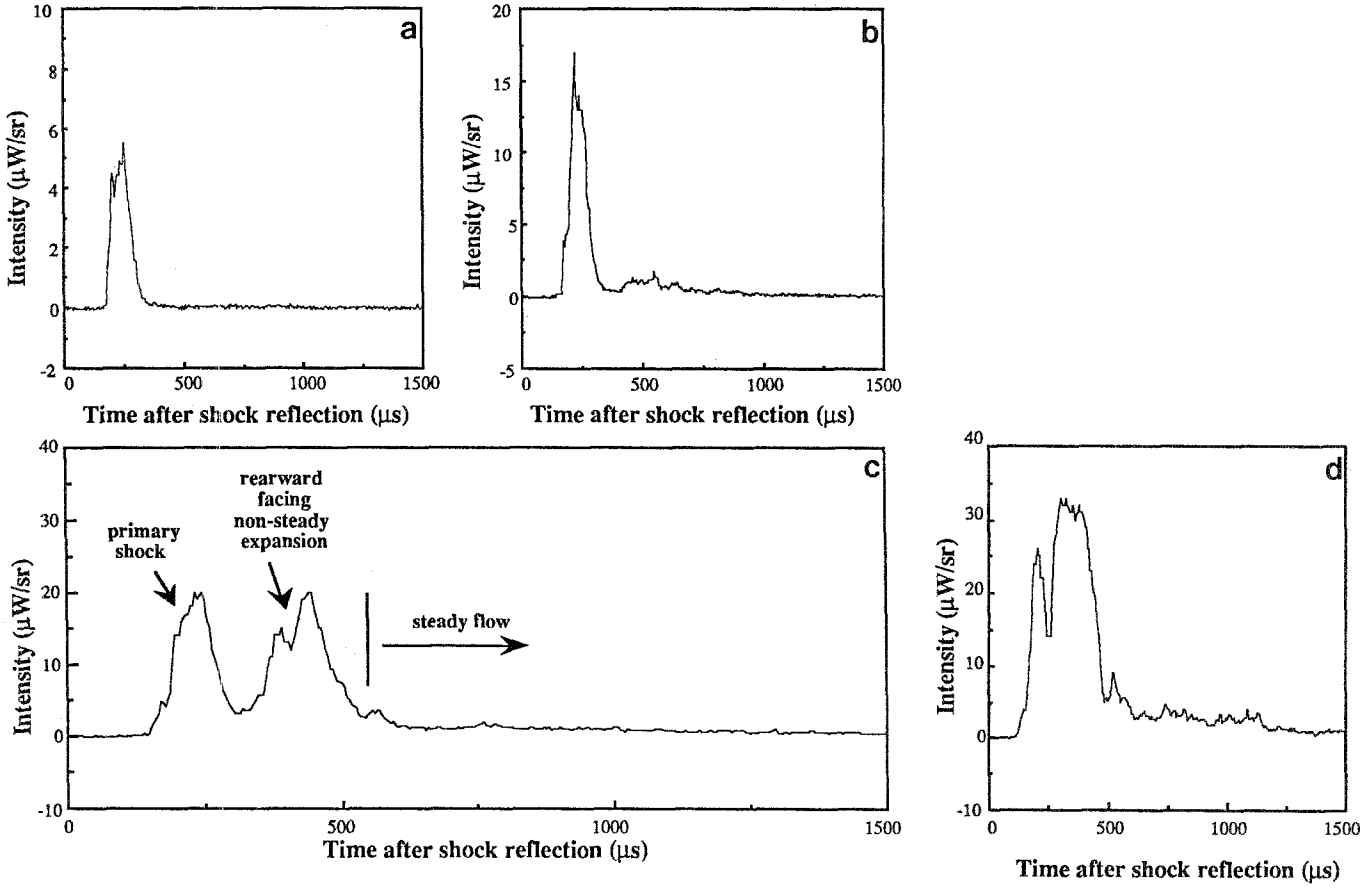

Fig. 3a–d. Variation of intensity with enthalpy for the 300.506 nm chromium line: **a** 8.3 MJ kg^{-1}; **b** 13 MJ kg^{-1}; **c** 17 MJ kg^{-1}; **d** 25 MJ kg^{-1}

JET. The observation region is 25 mm downstream of the brass injector.

Figure 3 shows the time resolved intensity of the chromium 300.506 nm line at various flow enthalpies. No signals were detected for the lowest enthalpy condition of 4.4 MJ kg^{-1}. Figure 3c illustrates the various details of the nozzle starting process (Smith 1966). Heat-transfer rate measurements performed by East, Stalker and Baird (1980) show a remarkable resemblance to the intensity measurements of Fig. 3c. The initial peak corresponds to the arrival of the primary shock followed closely by the recovery shock. The gradual increase in intensity between 300 and 450 μs after shock reflection is due to the rearward facing expansion wave. Finally, the intensity decreases due to development of boundary layers on the interior surfaces of the shock tunnel which decreases the rate at which impurities are introduced into the flow. The establishment of the nozzle flow stabilizes the flow temperature and this may also contribute to the decrease in intensity. This is followed by a period of steady flow which continues until the arrival of the helium driver gas (East et al. 1980). Figure 3d shows saturation of the photomultiplier at 45 μW sr^{-1}. Calibration showed that the photomultiplier was linear to at least 34 μW sr^{-1} and the OMA measurements indicate that the intensity may have been as high as 100 μW sr^{-1}.

The OMA results performed at 210 μs after shock reflection and at an enthalpy of 25 MJ kg^{-1} are shown in Fig. 4. The general background is found to be of the order of 1 mW sr^{-1} nm^{-1} between 290 and 330 nm. The two copper lines at 324.8 and 327.4 nm are the most prominent features of the spectrum. Measurements were also made at 400 and 800 μs after shock reflection for the 25 MJ kg^{-1} condition. Only the copper lines at 325 nm were detectable. The peak intensity of the 325 nm line was approximately 100 times less at 400 μs and approximately 200 times less at 800 μs. Therefore intensities during the steady flow period were several orders of magnitude less than those during the nozzle starting process and it is for this reason measurements were made during the starting process. Uncertainties after calibration were found to be approximately 10 % and 20 % for the OMA and photomultiplier results respectively.

4. Calculations

Detailed studies and calculations of fluorescence spectra for O_2 have been performed (Andresen et al. 1988; Lee and Hanson 1986; Kim et al. 1991). Here, for simplicity, we consider a tunable krypton fluoride excimer laser (248.0–248.9 nm) exciting one triplet component ($P_1(9)$, $v' = 2 \leftarrow v'' = 7$) at 248 nm and observing the fluorescence from one triplet component ($P_1(9)$, $v' = 2 \rightarrow v'' = 14$) at 325 nm.

For a laser pulse of duration t (sec), cross sectional area S (m^2) and spectral energy density ρ_ν (Jm^{-3}Hz^{-1}) at

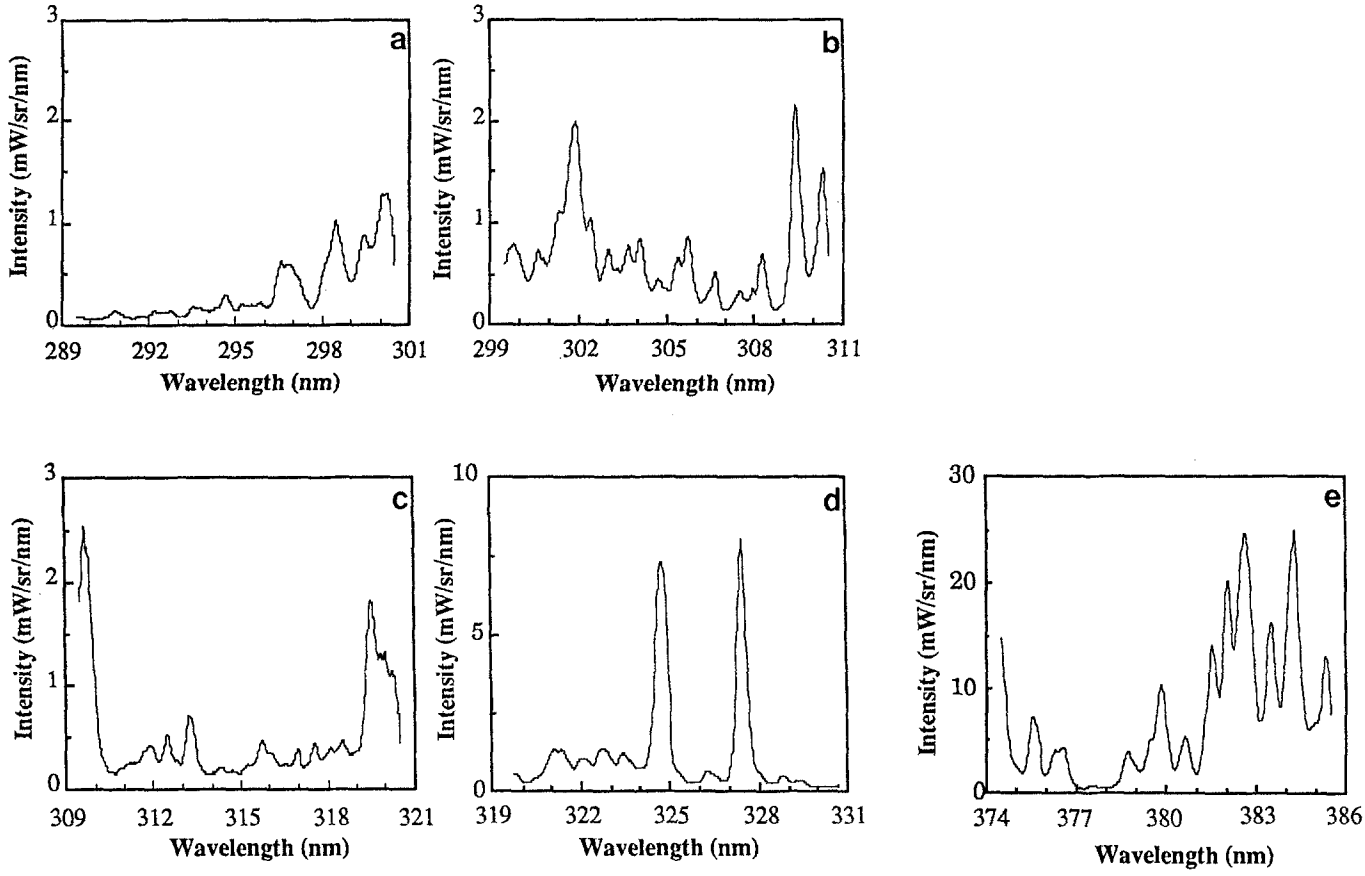

Fig. 4a–e. Absolute intensity measurements of background emissions at 25 MJ kg^{-1} and 210 μs after shock reflection. The OMA was positioned at the wavelengths: **a** 295 nm; **b** 305 nm; **c** 315 nm; **d** 325 nm; **e** 380 nm

frequency ν, the number of absorption transitions per laser pulse is $N\rho_\nu BtLS$. L (m) is the length of the absorbing medium and B ($s^{-1}(Jm^{-3}Hz^{-1})^{-1}$) is the absorption transition probability. N (m^{-3}) is the number density of the lower state ($\nu''J''$) for the absorption transition and is given from Boltzmann statistics to be

$$N = \frac{P}{kT}\frac{2J''+1}{Q_e Q_v Q_r}\exp\left\{\frac{hc}{kT}(T_e + G_{v''} + F_{J''})\right\} \quad (1)$$

where T (K) is the temperature and P (Pa) is the partial pressure of the absorbing species. Q_e, Q_v and Q_r are the electronic, vibrational and rotational partition functions respectively, while T_e, $G_{v''}$ and $F_{J''}$ are the electronic, vibrational and rotational energies of the lower state.

The fluorescence signal is determined by the fraction of the excited molecules which radiate via the particular emission transition. This fraction is given by $A_e/(\sum A_{v''J''} + Q_{pre} + Q_{cq})$ where A_e is the transition probability of the transition we are observing, $\sum A_{v''J''}$ is the sum of transition probabilities for all possible transitions from the excited state, and Q_{pre} and Q_{cq} are the predissociation and collisional quenching rates respectively. Since predissociation dominates all other de-excitation processes at pressures of the order of 1 atmosphere, $\sum A_{v''J''}$ and Q_{cq} are negligible when compared with Q_{pre}. The fluorescence signal (photons per steradian per laser pulse) is

$$F = \frac{1}{4\pi}N\rho_\nu BtLS\frac{A_e}{Q_{pre}} \quad (2)$$

The spectral energy density can be estimated by $E/(Stc\delta_\nu)$ where E (J) is the laser pulse energy, c (ms^{-1}) is the speed of light and δ_ν (Hz) is the laser linewidth. Substitution of this approximation into (2) eliminates the laser pulse duration t and cross sectional area S. For a sample of O_2 at 2000 K and a pressure of 0.21 atm, the number density of the lower state from (1) is $N = 2.72 \times 10^{18}$ molecules m^{-3}. Values used to calculate the partition functions and energy levels were found in Huber and Herzberg (1979). If $Q_{pre} = 7.35 \times 10^{10}\,s^{-1}$, $A_e = 3.98 \times 10^5\,s^{-1}$, $B = 1.47 \times 10^{18}\,s^{-1}(Jm^{-3}Hz^{-1})^{-1}$, $E = 650$ mJ, $\delta_\nu = 1.5 \times 10^{10}$ Hz and $L = 1$ cm, then from (2), $F = 2 \times 10^9$ photons sr^{-1} $pulse^{-1}$. The predissociation quenching rate was calculated from linewidths found in Lewis et al. (1986). Band transition probabilities and Hönl-London factors were from Allison et al. (1971) and Tatum (1966) respectively.

The background signal at 25 MJ kg^{-1} and 210 μs after shock reflection is approximately 7 mW sr^{-1} nm^{-1} at 325 nm (Fig. 3d). The LIF signal falls directly on the copper emission line at 325 nm. The number of background photons collected by the detector depends on the bandwidth of the detector (or filter) and the detector gating time. For a gate of 90 ns and filter of 1 nm bandwidth, the number of background photons emitted into 4π steradians is 1×10^9.

This gives a signal to background ratio of 2 to 1. This is a worst case situation since the background signal will be one to two orders of magnitude less when the experiment is performed at a more realistic enthalpy and flow time. The general background level at $25\,MJ\,kg^{-1}$ and $210\,\mu s$ was $1\,mW\,sr^{-1}\,nm^{-1}$. Further OMA results showed the intensities to be 100 times less at $400\,\mu s$ and $25\,MJ\,kg^{-1}$ and 20 times less at $210\,\mu s$ and $8.3\,MJ\,kg^{-1}$. The steady flow period, signified by a drop in background intensity, does not commence until about $400\,\mu s$ at $8\,MJ\,kg^{-1}$ which would make the signal to background ratio approximately 2000 to 1.

Andresen et al. (1988) have shown by experiments in an atmospheric flame that in most cases OH is the strongest emitter by a factor of 10 over transitions in the (0,6) band of O_2, and a factor of 100 for transitions in the (2,7) band of O_2. Hence careful selection of the LIF transition used and other experimental parameters (detector gating time, filter bandwidth) will significantly improve the signal to background ratio. LIF experiments in O_2 conducted on the ANU T2 free piston shock tunnel using a tunable argon fluoride excimer laser confirms these results (Sutton et al.).

5. Conclusions

In this experiment the absolute intensities of thermal emissions from a shock tunnel have been measured. A spectroscopic survey of the regions between 290 and 330 nm and 375 to 385 nm was conducted. Elements such as iron, chromium, nickel, molybdenum, copper, tin and aluminium were identified. These elements have been eroded from the surfaces exposed to the flow inside the shock tunnel. The variation of emission intensity with time was found to be due to the nozzle starting process. In general, the background in the 290 to 330 nm spectral region was found to be of the order of $1\,mW\,sr^{-1}\,nm^{-1}$ at $25\,MJ\,kg^{-1}$ and $210\,\mu s$ after shock reflection. A comparison with calculations of predissociated LIF signals from O_2 indicate a very favourable signal to background ratio. The background should be negligible for most LIF transitions unless the experiment is conducted during the nozzle starting process. One method used to reduce the impurities is to line the interior of the shock tube with copper (Hornung 1992). This removes the metallic impurities eroded from the shock tube walls at the expense of the few strong copper lines. Experiments involving the application of LIF to shock tunnels are continuing in this laboratory.

Acknowledgement. The authors would like to thank Paul Walsh for his expert operation of the shock tunnel and Paul Tant and Graeme Pike for their help in the construction of the experimental apparatus. P. Palma would like to express his sincere gratitude to David Pulford and Dr. S. Newman for their technical and experimental expertise. This work was funded by the Australian Research Council and NASA grant, NAGW 1467.

References

Allison AC, Dalgarno A, Pasachoff NW (1971) Absorption by vibrationally excited molecular oxygen in the Schumann-Runge continuum. Planet Space Sci 19:1463–1473

Andresen P, Bath A, Gröger W, Lülf HW, Meijer G, ter Meulen JJ (1988) Laser-induced fluorescence with tunable excimer lasers as a possible method for instantaneous temperature field measurements at high pressures: checks with an atmospheric flame. Appl Opt 27:365–378

East RA, Stalker RJ, Baird JP (1980) Measurements of heat transfer to a flat plate in a dissociated high-enthalpy laminar flow. J Fluid Mech 97:673–699

Hornung HG (1992) personal communication

Hornung HG, Sandeman RJ (1974) Interferometric measurements of radiating ionising argon flow over blunt bodies. J Phys D 7:920–934

Huber KP, Herzberg G (1979) Constants of diatomic molecules. Van Nostrand-Reinhold, New York

Kilpin D, Metal vapour contamination in high temperature shocks. To be published

Kim GS, Hitchcock LM, Rothe EW, Reck GP (1991) Identification and imaging of hot O_2 ($n'' = 2$, 3, or 4) in hydrogen flames using 193 nm- and 210 nm-range light. Appl Phys B 53:180–186

Lee MP, Hanson RK (1986) Calculations of O_2 absorption and fluorescence at elevated temperatures for a broadband argon-fluoride laser source at 193 nm. J Quant Spectrosc Radiat Transfer 36:425–440

Lewis BR, Berzins L, Carver JH, Gibson ST (1986) Rotational variation of predissociation linewidth in the Schumann-Runge bands of $^{16}O_2$. J Quant Spectrosc Radiat Transfer 36:187–207

Meier UE, Raiche GA, Crosley DR, Smith GP, Eckstrom DJ (1991) Laser-induced fluorescence decay lifetimes of shock-heated NO($A^2\Sigma^+$). Appl Phys B 53:138–141

Palmer JL, McMillin BK, Hanson RK (1992) Planar laser-induced fluorescence imaging of velocity and temperature in shock tunnel free jet flow. AIAA Paper 92-0762

Paul PH, Lee MP, Hanson RK (1989) Molecular velocity imaging of supersonic flows using pulsed planar laser-induced fluorescence of NO. Opt Lett 14:417–419

Pulford DRN, Newman DS, Houwing AFP, Sandeman RJ (1992) Coherent anti-stokes raman spectroscopy in a high enthalpy pulsed facility. IUTAM Symposium Marseille – Aerothermochemistry of Spacecraft and Associated Hypersonic Flows

Smith CE (1966) The starting process in a hypersonic nozzle. J Fluid Mech 24:625–640

Stalker RJ (1970) Shock tube developments at the Australian National University. Aust Physicist 7:99–102

Stalker RJ (1972) Development of a hypervelocity wind tunnel. Aero J of Roy Aero Soc 76:374–384

Stalker RJ, Morgan RG (1984) Supersonic hydrogen combustion with a short thrust nozzle. Combust Flame 57:55–70

Stalker RJ, Morgan RG, Netterfield MP (1988) Wave processes in SCRAMJET thrust generation. Combust. Flame 71:63–77

Sutton DJ, Houwing AFP, Palma PC, Sandeman RJ, Vibrational temperature measurements in a shock layer using laser induced predissociation fluorescence. Submitted to Shock Waves

Tatum JB (1966) Hönl-London factors for $^3\Sigma^{\pm} \rightarrow ^3\Sigma^{\pm}$ transitions. Can J Phys 44:2944–2946

This article was processed using Springer-Verlag TEX Shock Waves macro package 1.0 and the AMS fonts, developed by the American Mathematical Society.